**International Journal of Information, Engineering & Technology**
Volume 12, Issue 11, PP 60-67, ISSN: 2360-9194, September, 2025
OTL: 4272-1454-381-12116-1
Double Blind Peer Reviewed International Research Journal
**Journal Series: Global Academic Research Consortium (garc)**
arcnjournals@gmail.com
https://arcnjournals.com

# Optical and Photovoltaic Characterization of an Inverted P3HT:PCBM/ZnO Hybrid Solar Cell

**[1]*Ejikeme Ezo Igbokwe, [1]Anthony Kalu Uchechukwu, [2]Uchendu Timothy Ihekoronye**

[1]Department of Physics with Electronics, Ogbonnaya Onu Polytechnic, Aba, Nigeria
[2]Department of Civil Engineering, Ogbonnaya Onu Polytechnic, Aba, Nigeria

**Abstract:** *Hybrid solar cells combining organic and inorganic materials offer potential for low-cost, stable photovoltaics, but their optical and charge transport properties need further study. To characterize the optical properties and photovoltaic performance of an inverted P3HT:PCBM/ZnO hybrid solar cell with a laminated silver electrode. The device was fabricated using spray pyrolysis for ZnO, spin-coating for P3HT:PCBM and PEDOT:PSS, and lamination for the silver electrode. Optical properties were assessed via UV-Vis spectroscopy, and photovoltaic performance was evaluated under AM 1.5G illumination. P3HT:PCBM showed strong visible absorption (400–650 nm), while ZnO exhibited UV absorption and visible transparency. The device achieved Isc of 8.54 × 10⁻⁴ A, Voc of 0.578 V, FF of 0.68, and Pmax of 3.35 × 10⁻⁴ W. The inverted architecture demonstrates efficient light harvesting and charge extraction, with potential for cost-effective solar cells.*

**Keywords:** *Hybrid Solar Cell, P3HT:PCBM, ZnO, Inverted Structure, Photovoltaic performance.*

## Introduction

Hybrid solar cells, combining organic and inorganic materials, offer a promising pathway for developing low-cost, stable, and efficient photovoltaic devices. The blend of poly(3-hexylthiophene) (P3HT) and [6,6]-phenyl-C61-butyric acid methyl ester (PCBM) is widely utilized in organic solar cells due to its favorable morphology and efficient charge separation in bulk heterojunctions (Gines *et al*., 2007). Zinc oxide (ZnO), a wide-bandgap semiconductor, serves as an effective electron transport layer (ETL) owing to its high electron mobility and optical transparency in the visible spectrum (Minami, 2005). Inverted architectures, where the electron-collecting electrode is at the substrate, enhance device stability and simplify fabrication compared to conventional structures (Wang *et al*., 2016).

Despite progress, the synergistic effects of P3HT:PCBM and ZnO in inverted configurations, particularly with innovative electrode designs, remain underexplored. The use of laminated silver electrodes, which reduce fabrication complexity and cost compared to vacuum-deposited electrodes, has not been thoroughly investigated in such systems. This study addresses this gap by characterizing the optical properties (absorption and transmittance) and photovoltaic performance of an inverted P3HT:PCBM/ZnO hybrid solar cell with a laminated silver top electrode. The objectives are to evaluate the complementary optical properties of P3HT:PCBM and ZnO, assess the device's photovoltaic

parameters (short-circuit current, open-circuit voltage, fill factor, and maximum power output), and elucidate the role of the laminated electrode in enhancing stability and scalability.

## Materials and Methods

### Materials

Regioregular *poly(3-hexylthiophene-2,5-diyl)* (P3HT, >99%) and [6,6]-phenyl-C61-butyric acid methyl ester (PCBM, >99%) were sourced from Ossila Ltd. Indium tin oxide (ITO)-coated glass substrates (10 Ω/sq) served as bottom electrodes. Silver paste was used for laminated top electrodes. Zinc acetate dihydrate and diethanolamine were used for ZnO synthesis. PEDOT:PSS (Clevios™) acted as the hole transport layer. Analytical-grade solvents (toluene, acetone, methanol) and hydrochloric acid (37%) were used for substrate preparation.

### Device Fabrication

The inverted solar cell (ITO/ZnO/P3HT:PCBM/PEDOT:PSS/Ag) was fabricated as follows:

### Substrate Preparation

ITO-coated glass substrates were patterned using a plastic mask and etched with 37% HCl for 2 min at room temperature. Substrates were cleaned sequentially in toluene, acetone, and methanol (10 min each) via ultrasonication, then dried under nitrogen flow.

### ZnO Electron Transport Layer (ETL)

A ZnO precursor solution was prepared by dissolving 0.66 g zinc acetate dihydrate in 10 mL ethanol and 10 mL deionized water, stabilized with 0.5 mL diethanolamine under 30 min stirring. The solution was drop-cast onto ITO substrates and processed via spray pyrolysis at 300°C for 3 min to form a uniform ZnO film, following established protocols (Minami, 2005; Wang *et al*., 2016).

### Active Layer Deposition

P3HT and PCBM (0.6:1 weight ratio, 25 mg/mL in toluene) were dissolved and stirred overnight at 60°C in a nitrogen environment. The blend was spin-coated onto the ZnO layer at 2000 rpm for 20 s, then annealed at 100°C for 30 min to enhance crystallinity (Chirvase *et al*., 2004).

### Hole Transport Layer (HTL)

PEDOT:PSS was filtered (0.45 µm PVDF syringe filter) and spin-coated onto the active layer at 3000 rpm for 30 s, followed by drying at 100°C for 10 min.

### Top Electrode Application via Lamination

Silver paste was painted onto lamination paper and hot-pressed onto the PEDOT:PSS layer at 120°C for 30 s under gentle pressure, replacing vacuum evaporation to reduce fabrication complexity.

**Characterization**

Optical properties were measured using a UV-Vis spectrophotometer (200–800 nm). Photovoltaic performance was evaluated under AM 1.5G illumination (100 mW/cm²) with a calibrated solar simulator and source meter. Current-voltage (I-V) and power-voltage (P-V) curves were analyzed to determine short-circuit current density (Jsc), open-circuit voltage (Voc), fill factor (FF), and power conversion efficiency (PCE). Measurements were conducted under ambient conditions unless specified.

## Results and Discussion

Figure 1 shows the UV-Vis absorption spectra of the ZnO and P3HT:PCBM thin films. The results indicate that these materials exhibit distinct yet complementary optical properties, enhancing their functionality in hybrid solar cells. The P3HT:PCBM blend shows strong absorption in the visible region (400–650 nm), aligning with its role as the primary light-harvesting material in organic solar cells (Günes *et al*., 2007). In contrast, ZnO exhibits significant absorption in the UV region (below 400 nm), consistent with its wide bandgap (Minami, 2005). This spectral complementarity suggests that ZnO can contribute to improved device performance by capturing high-energy photons that P3HT:PCBM cannot utilize.

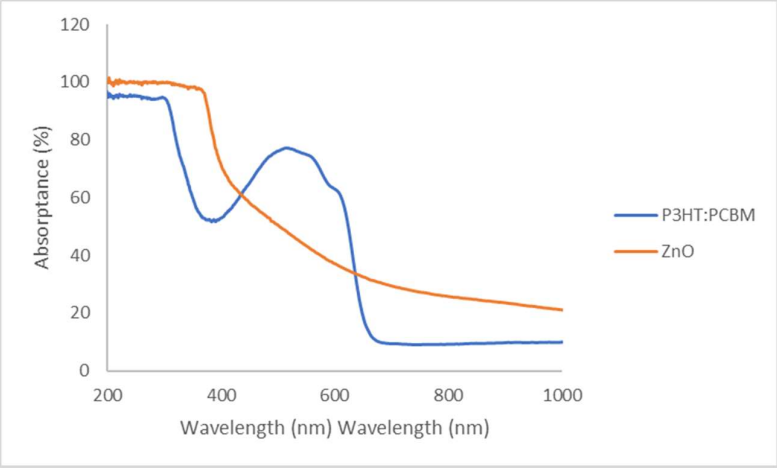


Figure 1: UV-Vis absorption spectra of ZnO and P3HT:PCBM thin films

Transmittance measurements (Figure 2) support these observations. The P3HT:PCBM film demonstrates low transmittance in the visible region, a consequence of its strong absorption and essential for effective solar energy conversion (Günes *et al*., 2007). ZnO, meanwhile, exhibits high transmittance across the visible range, a desirable property for electron transport layers (ETLs), which must remain optically transparent to avoid attenuating incoming light. Its strong UV absorption also indicates potential utility in filtering or absorbing high-energy photons that may otherwise degrade organic layers.

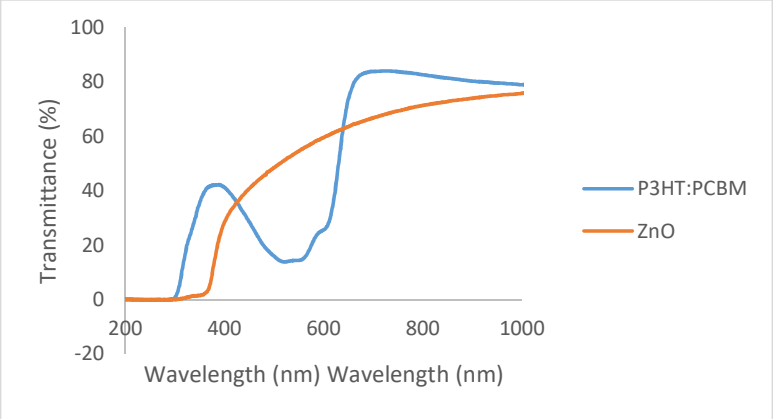


**Figure 2 Transmittance spectra of ZnO and P3HT:PCBM films**

These optical characteristics are in agreement with the fundamental electronic properties of the materials. P3HT:PCBM, a conjugated polymer blend, has a relatively narrow bandgap (~1.8–2.0 eV), whereas ZnO is a wide bandgap semiconductor (~3.3 eV), which explains its transparency in the visible region (Minami, 2005).

The absorption coefficient (α) is a critical parameter in solar cell design as it dictates how effectively light can be harvested within the active layer. Figure 3 compares the absorption coefficients of P3HT:PCBM and ZnO. The high α of P3HT:PCBM in the visible region enables efficient exciton generation under solar illumination (Günes *et al.*, 2007). Conversely, ZnO's high α in the UV region contributes to UV light harvesting and may also serve to enhance photogenerated current in hybrid systems.

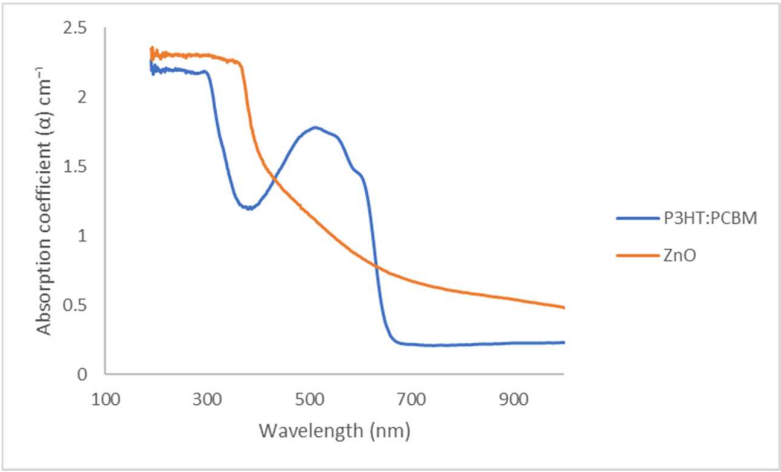


**Figure 3 Absorption coefficient spectra of ZnO and P3HT:PCBM**

Figure 4 displays the extinction coefficient (k) spectra for both P3HT:PCBM and ZnO. The extinction coefficient, which represents the attenuation of light due to absorption and scattering, directly correlates with the material's ability to absorb light. P3HT:PCBM demonstrates a pronounced peak in the visible range around 500 nm, which directly aligns with its strong absorption behavior observed in the absorption spectra. Beyond 600 nm, the extinction coefficient of P3HT:PCBM diminishes progressively, indicating lower attenuation of light at longer wavelengths. Conversely, ZnO shows a steep rise in its extinction coefficient below 380 nm, corresponding precisely to its absorption edge in the UV region. In the visible range, the extinction coefficient of ZnO remains significantly lower than that of P3HT:PCBM. These results vividly reflect the spectral dependence of light attenuation in each

material. They further reinforce the functional distinction between the layers: P3HT:PCBM serves as the primary light-harvesting medium in the visible region, while ZnO fulfills a complementary role by attenuating UV radiation and remaining largely transparent to visible light, thereby facilitating light penetration to the active layer.

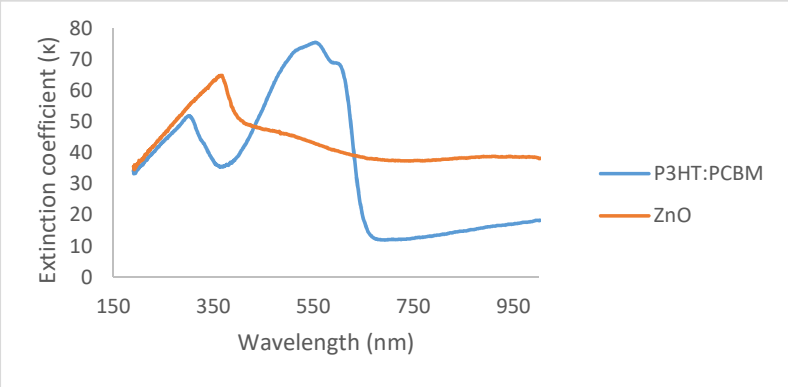


**Figure 4 Extinction coefficient for P3HT:PCBM and ZnO**

**Photovoltaic Performance and Device Physics**

The inverted device architecture employed in this study, with ZnO serving as the ETL, offers several significant advantages over conventional structures. Firstly, the use of ZnO can enhance device stability, as ZnO is known for its robustness compared to some traditional organic ETLs. Secondly, the inverted configuration can simplify the fabrication process and improve compatibility with various substrates (Wang *et al*., 2016).

Figure 5 illustrates the layer configuration of the fabricated hybrid solar cell, which adopts an inverted structure. The device is composed of the following layers arranged sequentially: Glass substrate / ITO / ZnO / P3HT:PCBM / PEDOT:PSS / Silver / Lamination Plastic.

The glass substrate serves as the base for mechanical stability. The ITO layer, a transparent conducting oxide, functions as the electron-collecting electrode in this configuration. ZnO is deposited atop the ITO and serves as an electron transport layer (ETL), enabling efficient electron extraction and hole blocking. The active layer, P3HT:PCBM, is a bulk heterojunction composed of donor (P3HT) and acceptor (PCBM) materials responsible for photon absorption and exciton generation.

PEDOT:PSS is applied as the hole transport layer (HTL) to facilitate hole extraction from the active layer. A silver layer is used as the top electrode for hole collection. Finally, a lamination plastic layer is applied for device encapsulation and environmental protection. In this inverted setup, electron collection occurs at the ITO electrode and hole collection at the silver electrode.

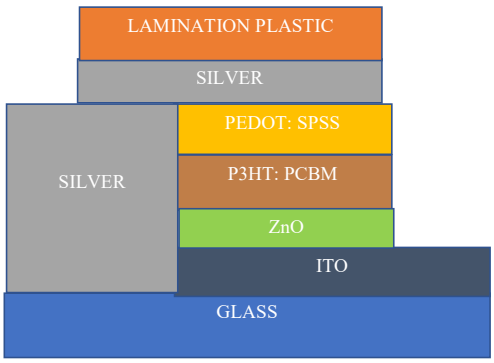


**Figure 5 Device Structure of the Solar Cell**

The overall efficiency of this photovoltaic process is critically dependent on several factors, including the light absorption characteristics of the active layer, the effectiveness of exciton dissociation and charge separation, the efficiency of charge transport pathways, and the quality of the contacts at the electrodes.

The current-voltage (I-V) and power-voltage (P-V) characteristics of the fabricated solar cell under AM 1.5G illumination are presented in Figure 6. Table 1 summarizes the extracted key photovoltaic parameters.

The current–voltage (I–V) and power–voltage (P–V) characteristics of the fabricated P3HT:PCBM/ZnO hybrid solar cell under standard AM 1.5G illumination (100 mW/cm²) are presented in Figure 7. These curves reveal the operational behavior of the device and provide insight into its charge separation and power generation capabilities.

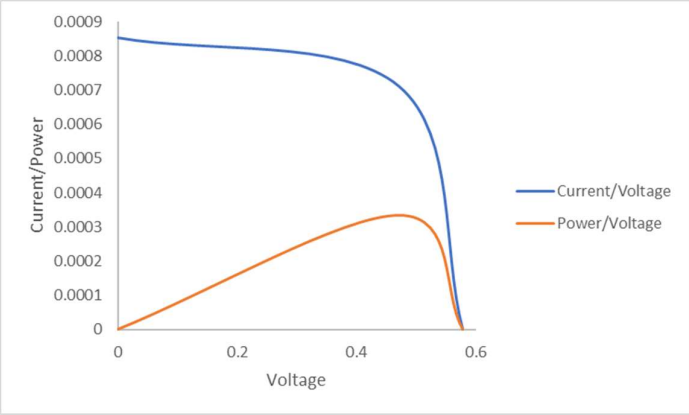


**Figure 6 I–V and P–V curves of the fabricated P3HT:PCBM/ZnO hybrid solar cell**

The I–V curve displays a typical diode-like profile, confirming photovoltaic activity. A well-defined short-circuit current (Isc) of $8.54 \times 10^{-4}$ A and an open-circuit voltage (Voc) of 0.578195 V were recorded. These values are indicative of efficient photo-induced charge generation and separation within the device (Nelson, 2003).

The P–V curve shows a distinct peak corresponding to the maximum power point (Pmax), which was determined to be $3.35 \times 10^{-4}$ W, occurring at a voltage of 0.471511 V and a current of $7.11 \times 10^{-4}$ A. These results confirm the device's capability to operate efficiently under illumination, translating incident solar energy into usable electrical power.

The photovoltaic parameters derived from the I–V curve are summarized in Table 1. The fill factor (FF) was calculated to be 0.68, reflecting a relatively high degree of squareness of the I–V curve and suggesting minimal resistive losses and reasonably effective charge transport. Though satisfactory, this FF indicates some scope for further optimization in terms of series resistance and carrier recombination (Brabec *et al.*, 2001).

**Table 1 Summary of photovoltaic performance parameters including Voc, Isc, FF, and Pmax**

| Characteristics | ZnO/P3HT:PCMB |
|---|---|
| Voc | 0.578195 |
| Isc | 8.54E-04 |
| Vmax | 0.471511 |
| Imax | 0.00071137 |
| FF | 0.68 |
| Pmax | 3.35E-04 |
| H | 2.096 |

The overall performance of the device is largely influenced by several interconnected factors, including the optical absorption capabilities of the P3HT:PCBM active layer, the effective charge extraction facilitated by ZnO as an electron transport layer (ETL), and the interfacial properties of the electrode contacts. The strong absorption and high extinction coefficient of P3HT:PCBM in the visible region, discussed earlier, contribute directly to the observed high Isc (Green *et al.*, 2021). Additionally, the favorable energy level alignment and wide bandgap of ZnO allow for effective electron transport while maintaining transparency in the visible range.

These results validate the design strategy of incorporating ZnO as an ETL and demonstrate the feasibility of using a P3HT:PCBM-based hybrid architecture for low-cost photovoltaic applications.

## Conclusion

This study characterized the optical and photovoltaic performance of an inverted P3HT:PCBM/ZnO hybrid solar cell with a laminated silver electrode. The P3HT:PCBM active layer exhibited strong absorption in the visible spectrum (400–650 nm), enabling efficient light harvesting, while ZnO demonstrated high transparency in the visible range and significant UV absorption, supporting its role as an effective electron transport layer. Photovoltaic evaluation revealed a short-circuit current (Isc) of $8.54 \times 10^{-4}$ A, open-circuit voltage (Voc) of 0.578 V, fill factor (FF) of 0.68, and maximum power output (Pmax) of $3.35 \times 10^{-4}$ W, confirming efficient charge separation and collection. The laminated silver electrode enhanced stability and simplified fabrication, demonstrating the potential of this inverted architecture for low-cost photovoltaic applications. Future optimization of active layer thickness and interface engineering is recommended to further improve power conversion efficiency.

**References**

Brabec, C. J., Sariciftci, N. S., & Hummelen, J. C. (2001). Plastic solar cells. **Advanced Functional Materials**, *11*(1), 15–26. https://doi.org/10.1002/1616-3028(200102)11:1<15::AID-ADFM15>3.0.CO;2-A

Chirvase, D., Parisi, J., Hummelen, J. C., & Dyakonov, V. (2004). Influence of nanomorphology on the photovoltaic action of polymer–fullerene composites. **Nanotechnology**, *15*(9), 1317–1323. https://doi.org/10.1088/0957-4484/15/9/013

Gines, S., Neugebauer, H., & Sariciftci, N. S. (2007). Conjugated polymer-based organic solar cells. **Chemical Reviews**, *107*(4), 1324–1338. https://doi.org/10.1021/cr050149z

Green, M. A., Dunlop, E. D., Hohl-Ebinger, J., Yoshita, M., Kopidakis, N., & Hao, X. (2021). Solar cell efficiency tables (Version 58). **Progress in Photovoltaics: Research and Applications**, *29*(7), 657–667. https://doi.org/10.1002/pip.3371

Minami, T. (2005). Transparent conducting oxide semiconductors for transparent electrodes. **Semiconductor Science and Technology**, *20*(4), S35–S44. https://doi.org/10.1088/0268-1242/20/4/004

Nelson, J. (2003). *The physics of solar cells*. World Scientific Publishing.

Wang, K., Liu, C., Meng, T., Yi, C., & Gong, X. (2016). Inverted organic photovoltaic cells. **Chemical Society Reviews**, *45*(10), 2937–2975. https://doi.org/10.1039/C5CS00831J